Triplet-Triplet Annihilation Upconversion with Reversible Emission-Tunability Induced by Chemical-Stimuli

Yaxiong Wei, Haitao Xian, Xialei Lv, Fan Ni, Xiaosong Cao and Chuluo Yang**

Dr. Y. Wei, H. Xian, Dr, X. Lv, Dr F. Ni, Dr. X. Cao, Prof. C. Yang
Shenzhen Key Laboratory of Polymer Science and Technology, College of Materials Science and Engineering
Shenzhen University
Shenzhen 518060, China
E-mail: clyang@szu.edu.cn

Dr. Y. Wei, Dr, X. Lv, Dr F. Ni
College of Physics and Optoelectronic Engineering
Shenzhen University
Shenzhen 518060, China

Keywords: Triplet-triplet annihilation upconversion, reversible color-tunable, Os(II) complexes, geometric isomerism.

TOC

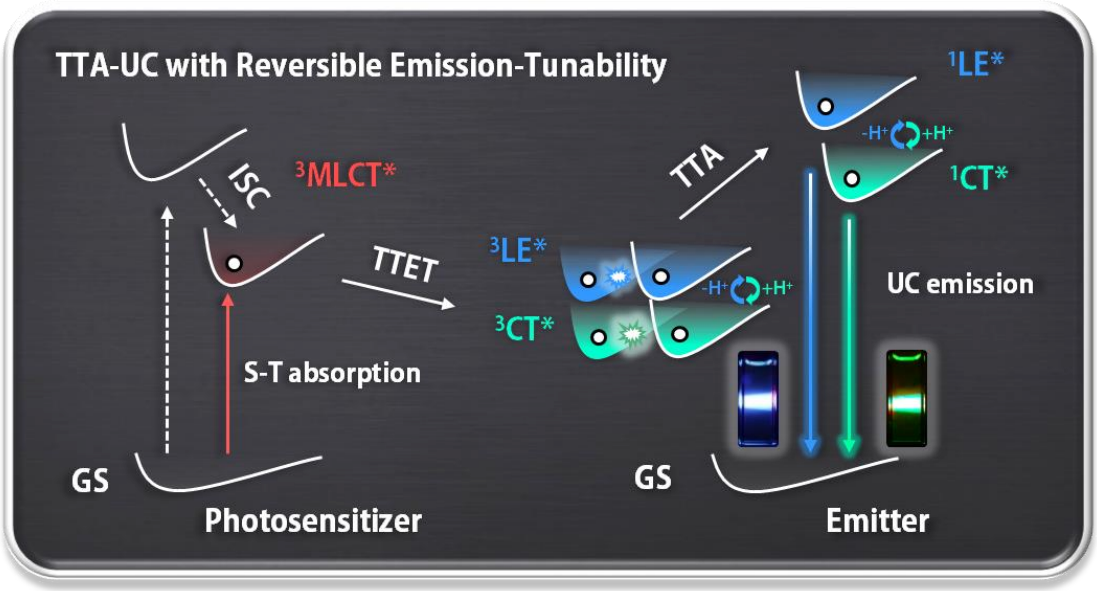

Abstract

Triplet-triplet annihilation upconversion (TTA-UC) has been widely studied, but color-tunable TTA-UC system triggered by chemical stimuli has not yet been proposed. Herein, reversible acid/base switching of TTA-UC emission wavelength is achieved for the first time by a simple platform, composed of a direct singlet-triplet (S-T) absorpting photosensitizer, and pH-responsive 9,10-bipyridineanthracene (DPyA) as acceptor. The sensitizer-acceptor pair exhibits efficient UC emission (quantum yield up to 3.3%, anti-Stokes shift up to 0.92 eV) with remarkable contrast upon base/acid treatment ($\Delta\lambda_{em,max}$ = 82 nm, 0.46 eV). In a proof-of-concept study, the color-adjustable UC emission was applied as a remote modulator to photo-control reversible chemical reactions for the first time. This platform enriches the portfolio of color-switchable TTA-UC, and the mechanism would inspire further development of smart UC systems and extend the application field of upconversion.

Triplet-triplet annihilation upconversion (TTA-UC) is highly promising in various UC techniques due to low power density requirement, adjustable excitation/emission wavelength and high UC quantum yield.[1] The past few decades have witnessed the development and utilization of plenty of photosensitizers/acceptors in TTA-UC with quantum efficiency exceeding 40% and anti-Stokes shift as high as 1.27 eV.[2] Appealing applications in photovoltaics,[3] photocatalysis,[4] photoelectrochemistry,[5] organic light emitting diode,[6] circularly polarized luminescence[7] have been correspondingly proposed and studied. In particular, TTA-UC has unique advantages in biological fluorescent sensing, enabling visible imaging of deeper layers by near-infrared (NIR) excitation with strong penetrability.[8]

Introduction of stimuli responsiveness into TTA-UC furtherly broadens the application of UC system by modulating the triplet and/or singlet manifolds of acceptors. Since the very first demonstration that reversible ON/OFF photo-switching of TTA-UC could be realized by quenching/regenerating the excited states,[9] the sources of available external stimuli for ON-OFF switching TTA-UC have been quickly enriched, including light, oxidant, metal ion, stress, temperature, etc.[10] On the other hand, the color-tunable TTA-UC emission under single-wavelength excitation is undoubtedly more favorable for remote control of molecular photo-switching reactions, multiplexed detection and multicolor imaging, but with much less examples hitherto.[11] The major challenge is to realize a recognizable emission change between different states of the acceptor, yet not interfering with the TTA-UC process. Kimizuka et al have designed a new asymmetric luminescent cyclophane acceptor

with switchable emission characteristics to realize reversible emission color switching of TTA-UC by different crystalline structures.[11a] More recently, Han et al and Li et al reported color-tunable TTA-UC by fluorescence chromophores with solvatochromism effect.[11b, 11c] Despite the considerable progresses, the current platforms merely rely on phase/solvent change and all exhibit low-contrast ($\Delta\lambda_{em,max} \leq 50$ nm), which become the major limitations to further applications.

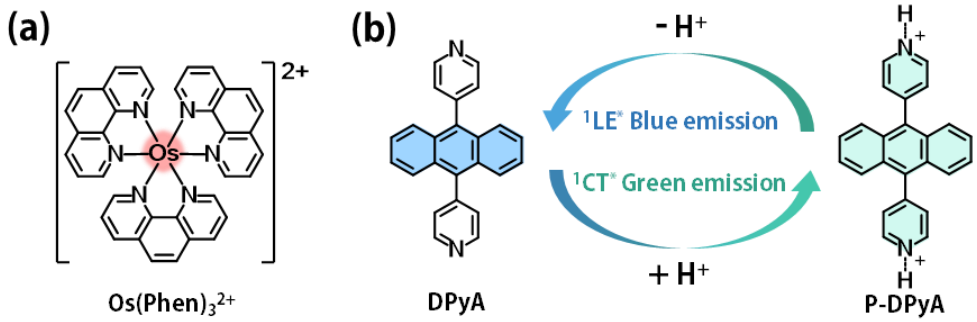

Scheme 1. (a) The molecular structures of the deep-red absorption photosensitizer Os(phen)$_3^{2+}$. (b) The mechanism of reversable color-switched with acceptor DPyA, the emission color can be switched between deep-blue and green by the acid/base.

In this context, we showcase the first TTA-UC platform with reversible color-tunable emission in situ by chemical stimuli (acid/base), simply composed by a deep-red/ NIR absorption photosensitizer Os(phen)$_3^{2+}$ and a pyridine-derived pH-responsive acceptor (**Scheme 1a**). The weakly alkaline pyridine moiety with moderate electron accepting capability becomes strongly electron deficient once get protonated, and could therefore serve as an ideal modulator for emissive color. By extending this mechanism, 9,10-dipyridineanthracene (DPyA), a pyridine-containing analogous of the traditionally acceptor 9,10-diphenylanthracene (DPA), was accessed. The fluorescence shows local

excited (LE) deep-blue fluorescence emission. Meanwhile, the protonated DPyA (P-DPyA) shows charge transfer (CT) green emission (**Scheme 1b**). When DPyA was used as triplet acceptor for TTA-UC and excited by deep-red laser, the reversible acid-base TTA-UC emission exchange could be easily identified by naked eyes with stokes shift up to 82 nm. The UC system with tunable emission was subsequently exploited as a light source to photocontrol chemical reaction.

The absorption and fluorescence spectra of DPyA in solution were analogous to DPA (**Figure S3**), with three π-π* absorption bands peaking at 356 nm, 374 nm, 394 nm and two emission peaks at 417 nm and 430 nm (**Figure 1a-b, Table 1**). Upon titration of trifluoroacetic acid (TFA), the absorption intensity of DPyA was gradually decreased with broadening bands (**Figure 1a**). Concurrently, distinct acidochromism with subsided deep-blue fluorescent emission and newly emerged structureless green emission band (499 nm) was noticed (**Figure 1b**). The protonated pyridine acted as strong acceptor in DPyA that produce the CT green emission and $\Delta\lambda_{em,max}$ up to 82 nm. The absolute fluorescence quantum yields (Φ_{PL}) were 85% and 30% for DPyA and P-DPyA, respectively. Meanwhile, time-resolved emission spectra (TRES) were recorded to study the fluorescence lifetime (**Figure 1c-d**). The fluorescence dynamics show a single-exponential decay (**Figure S5**) and the lifetime was determined to be 6.5 ns (430 nm) for LE emission of DPyA and 5.9 ns (510 nm) for CT emission of P-DPyA, indicating that only one excited state was involved in each fluorescence band (**Table 1**).

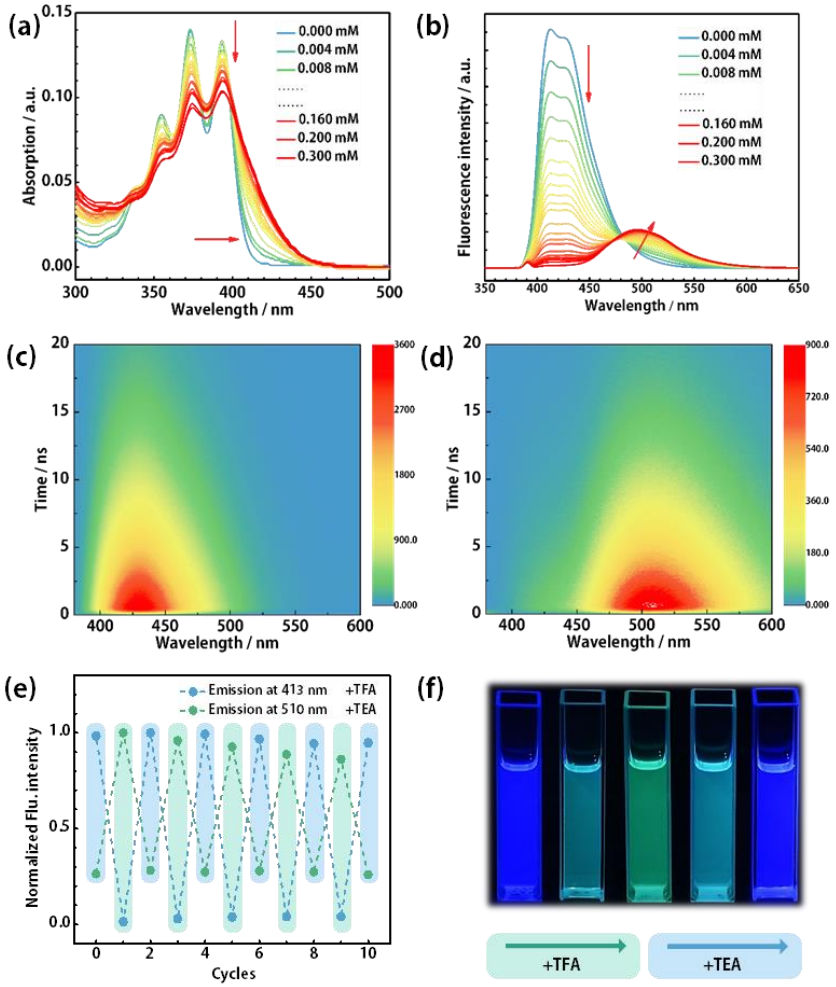

Figure 1. (a) The absorption spectra of DPyA with different concentration of TFA; (b) The emission spectra of DPyA with different concentration of TFA; (c-d) Time-resolved emission spectra of DPyA in absence or presence of TFA, λ_{ex} = 390 nm. c[DPyA] = 1×10^{-5} M; (e) The reversibility of the acid-base switching of fluorescence of DPyA; (f) The photographs of acid-base switching of fluorescence upon excitation with 365 nm light. Trifluoroacetic acid (TFA) as acid, triethylamine (TEA) as base, 1,2-dichloroethane as solvent.

The reversibility of acid/base responsiveness was subsequently tested (**Figure 1e**). Under photoexcitation at 390 nm, the intense deep-blue (417 nm) fluorescence of DPyA quickly bathochromic-shifted into sky-blue and then green region upon gradual addition of TFA. Adding equivalent amount of triethylamine (TEA) relative to TFA

would alter the fluorescence from green back to deep-blue immediately. The whole process could be clearly visualized by naked eyes (**Figure 1f**), and there existed no significant changes in emission intensity within several experimental cycles (**Figure S6**). These results clearly suggested that DPyA experince efficient and reliable acid/base induced bi-color switching with negligible interference of trifluoroacetate salt, even at relative high concentration. Similar pH-switched fluorescence has been reported to work well in *vivo* imaging of cells.[12]

To further unveil the origin of photophysical differences between DPyA and P-DPyA, density functional theory (DFT) and time-dependent density functional theory (TD-DFT) calculations were carried out at B3LYP/6-31G level. As detailed in **Figure S7**, the DPyA adopted a fully orthogonal configuration with 90.0° dihedral angles between pyridine moieties and anthrancene. Since the frontier molecular orbitals were centered at the anthracene unit, the fluorescence was thereby rationalized as LE emission, and the first singlet excited state energy (S_1) was 3.13 eV (c.a. 400 nm) with considerable oscillator strength (f = 0.1814). After protonation, the HOMO remained on anthracene unit, while the LUMO largely resided on the electron-deficient pyridinium subunits, with decreased dihedral angles to 68.1°. Correspondingly, the fluorescence showed CT-character with more stabilized S_1 at 2.06 eV and reduced f of 0.1231. The triplet spin density surfaces of DPyA were localized in anthracene segment and the triplet state energy level was determined to be 1.74 eV, while that of the P-DPyA was distributed on the whole molecule, and that's the delocalization energy of triplet states was also decreased and the triplet state energy level slightly lowered to

1.54 eV. The theoretical calculations coincided well with the experimental results.

Table 1. The photophysical parameters of photosensitizer and acceptor

Compound	λ_{Abs} / nm	λ_{Em} / nm	Φ_{FL} / %	τ / ns	T_1 / eV	k_q /10^9 M^{-1}•s^{-1}	Φ_{UC} / %
$Os(phen)_3^{2+}$	432/481	690	5.5	290	1.80[a]	-	-
DPyA	356/374/394	417/430	85	6.5	1.74[b]	0.51	3.3
P-DPyA	357/374/394	499	30	5.9	1.54[b]	0.30	0.5

[a] Calculated with the phosphorescence emission peak; [b] The DFT calculated values.

The $Os(phen)_3^{2+}$ (**Scheme 1a**) was selected as the photosensitizer due to its appropriate triplet state energy (T_1 = 1.80 eV)[2c, 2d] for sensitizing the DPyA (T_1 = 1.74 eV) and P-DPyA (T_1 = 1.54 eV). The small triplet energy level differences between photosensitizer and acceptors (ΔE_{TTET} = 0.06 eV) were slightly greater than zero that is beneficial to obtain simultaneously large anti-stoke shift and high triplet-triplet energy transfer (TTET) efficiency. The TTET between $Os(phen)_3^{2+}$ and DPyA were investigated by monitoring phosphorescence of the sensitizer in different concentration of the acceptor. As illustrated in **Figure 2a**, the phosphorescence lifetime (τ_{Ph}) of $Os(Phen)_3^{2+}$ was determined as 0.29 μs and decrease to 0.12 μs in the presence of 10 mM DPyA, indicating effective TTET process between $Os(Phen)_3^{2+}$ and DPyA. In a similar manner, quenching of phosphorescence was observed with the presence of P-DPyA (**Figure 2b**), and the τ_{Ph} of $Os(Phen)_3^{2+}$ was reduced to 0.15 μs. The bimolecular quenching rates (k_q) could be therefore deduced by the Stern-Volmer quenching curves

of $Os(Phen)_3^{2+}$ phosphorescence lifetime vs concentration of the acceptor (**Figure 2c**) to be 0.51×10^9 $M^{-1}\bullet s^{-1}$ for DPyA and 0.30×10^9 $M^{-1}\bullet s^{-1}$ for P-DPyA, with both TTET efficiencies exceeding 50%. The smaller k_q and slightly decreased TTET efficiency acquired in $Os(phen)_3^{2+}$/P-DPyA system could be explained by their mutual coulomb repulsion that lowered the chance for direct collision between sensitizer and acceptor.

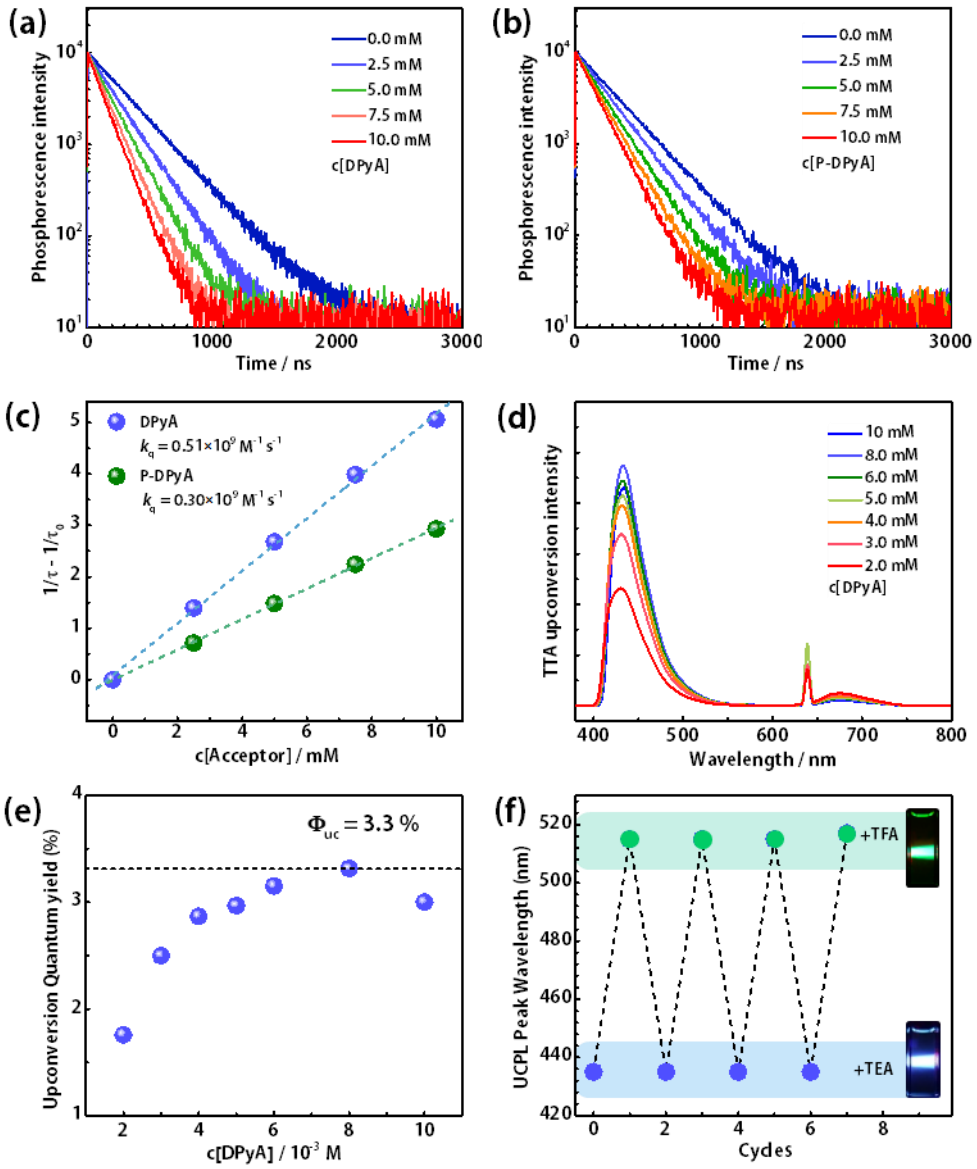

Figure 2. (a) Variation of phosphorescence lifetime of $Os(Phen)_3^{2+}$ with concentration of DPyA; (b) Variation of phosphorescence lifetime of $Os(Phen)_3^{2+}$ with concentration of P-DPyA; λ_{ex} = 640 nm. (c) The bimolecular quenching rate generated from the

phosphorescence lifetime quenching curves. (d) Upconverted fluorescence emission spectra in different concentration of DPyA, shortpass filter at 635 nm; (e) Effect of DPyA concentration on TTA upconversion quantum yield; (f) The reversibility of the acid-base switching of upconversion emission wavelength. 1,2-dichloroethane as the solvent, c[$Os(Phen)_3^{2+}$] = 1×10^{-5} M, λ_{ex} = 638 nm.

The TTA-UC properties were subsequently tested in degassed 1,2-dichloroethane. When irradiated by a 638 nm continuum light, the strong blue UC emission was observed at 433 nm (**Figure 2d**), while no blue emission could be detected in the absence of $Os(Phen)_3^{2+}$. The UC intensity increased rapidly and then trended to be stable when DPyA concentration was greater than 6 mM, accompanying by faded $Os(Phen)_3^{2+}$ phosphorescence (λ_{max} = 690 nm). The highest Φ_{UC} values achieved with 8 mM of DPyA was 3.3% (set the maximum UC quantum yield at 100%), and obvious parasitic self-absorption emerged at higher concentration with decreased Φ_{UC} (**Figure 2e**). As expected, the blue UC emission bathochromic-shifted immediately (λ_{max} = 515 nm) by excessive TFA treatment (Φ_{UC} = 0.5%), in high consistency with the fluorescent change of acceptor under direct photoexcitation, hinting the involvement of same excited states (**Figure S8**). This, of course, was also guaranteed by the decent stability of $Os(Phen)_3^{2+}$ in excessive acid as suggested by unaltered UV-Vis absorption spectra and phosphorescent lifetime (**Figure S9-S10**). Interestingly, after deprotonation with base, the blue UC emission was completely restored with no significant change of intensity (**Figure S8**). As shown in **Figure 2f**, the reversible switching of TTA-UC was clearly discernable, and remained stable for several repetitive cycles.

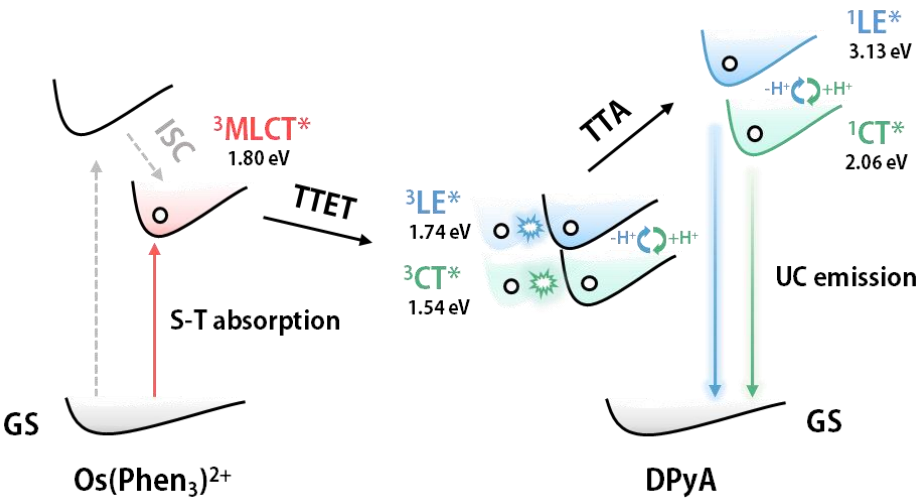

Scheme 2. Jablonski diagram of the TTA-UC process between $Os(Phen_3)^{2+}$ and DPyA, where GS stands for ground state; ^{3}MLCT* represents the metal-to-ligand charge-transfer triplet excited state of $Os(Phen^3)^{2+}$. TTA-UC emission could be adjusted from 433 to 515 nm reversibly by simple protonation/deprotonation of DPyA acceptor.

The mechanism of the TTA-UC was clearly pictured in **Scheme 2**. Since $Os(Phen)_3^{2+}$ possessed singlet-to-triplet (S-T) transition absorption, the T_1 state of Os complex was directly accessed under irradiation of low-energy light at initial stage, minimizing the energy loss for triplet sensitization by omitting the intersystem crossing (ISC) from S_1 to T_1. The use of 638 nm laser was merely due to the restriction of available excitation light source. Subsequently, the T_1 of either DPyA or P-DPyA was activated via diffusion controlled Dexter energy transfer, followed by collision-induced TTA between two triplet molecules to generate a higher-energy photon. The direct S-T absorption and adequate ΔE_{TTET} between photosensitizer and acceptors ensured large energy gain (up to 0.92 eV), while the $*LE^1$ to $*CT^1$ switch between DPyA and PD-

DPyA allowed a 0.46 eV adjustment of the stimuli-responsive TTA-UC emission. The causes for Φ_{UC} difference between $Os(phen)_3^{2+}$/DPyA (3.3%) and $Os(phen)_3^{2+}$/P-DPyA (0.5%) were multifold, involving the TTET, TTA and fluorescence emission (FL) process. For the downward TTET and FL process, the $Os(phen)_3^{2+}$/P-DPyA pair showed slightly inferior TTET efficiency (mainly ascribing to bimolecular repulsion between positive-charged photosensitizer and acceptor) and lower quantum yield. While in the upward TTA step, the energy gap between the singlet state and twice of the triplet state, *i.e.* $\Delta E_{TTA} = 2\times E(T_1)\text{-}E(S_1)$ for DPyA (0.35 eV) was also significantly smaller than that of P-DPyA (1.02 eV).[13] Further enhancement of Φ_{UC} could be realized by selecting a neutral or oppositely-charged sensitizer and improving the quantum yield of acceptor in both forms via delicate molecular design.

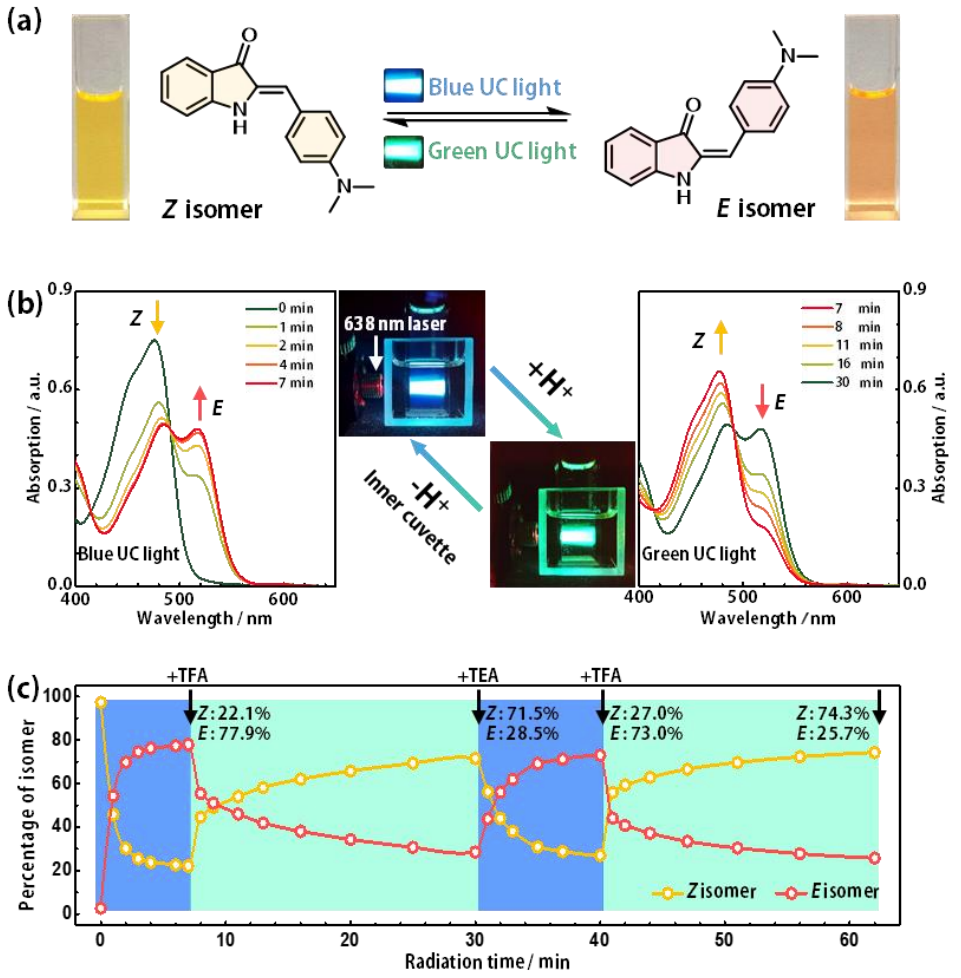

Figure 3. (a) The hemiindigos molecular configuration of Z isomer and E isomer and color photos of solutions; (b) The absorption spectra changes of hemiindigos molecular under photoexcitation at 638 nm; (c) The reversible between Z isomer and E isomer with the reversible upconversion system.

The red/NIR-to-visible triplet fusion system with adjustable UC emission is highly valuable for advanced chemical, biological and environmental applications. Notably, the absorption band of $Os(Phen)_3^{2+}$ extends to NIR light (over 700 nm) and falls into the first biological transparency windows[14]. Herein, the TTA-UC platform was adopted for the first time to induce reversible chemical changes under low-energy light

excitation at fixed wavelength. Specifically, the photo-isomerization of a hemiindigo derivative 2-(4-(dimethylamino)benzylidene)indolin-3-one (**Figure 3a**), with interchangeable isomeric state upon blue/green light excitation ($Z \rightarrow E$ switching occurred at 440 nm and $E \rightarrow Z$ switching at 520 nm, **Figure S11**), was selected as the proof-of-concept reaction owing to its perfect adaption with our TTA-UC system and distinct photochromism of each individual isomeric states according to a recent report by Dube et. al.[15]. It is noteworthy that the ability changes in spectral absorption is of particular importance for applications in energy storage and chemical sensing and for controlling the conformation and activity of biomolecules[15-16].

By immersing the inner cuvette containing unacidified TTA-UC system in the hemiindigo solution, the geometry switching from *Z* to *E* states occurred efficiently as promoted by strong UC blue emission (435 nm) under photoexcitation at 638 nm (**Figure 3b**), giving 77.9% *E* isomer at photostationary state (pss). Excessive TFA addition to the inner cuvette changed the UC emission to green immediately (λ_{max} = 515 nm) and switched *E* to *Z* direction, reaching 71.5% *Z* isomer at pss. The dual state photoswitching of hemiindigo manifested decent reversibility by color-tunable UC photoexcitation (**Figure 3c and Figure S13)**. Control experiment in which the TTA-UC system was removed showed only trace yields of opposite isomer upon continuous photoexcitation at 638 nm (**Figure S12**).

To sum up, we have constructed a pyridine-anthracene conjugate as acceptor, and achieved reversible in situ color-tunable TTA-UC system upon chemical stimuli for the first time. Utilization of the S-T absorption photosensitizer enabled a large anti-Stokes

shift from deep-red to blue/green emission with UC quantum yield up to 3.3%. Importantly, the UC emission wavelength of $Os(Phen)_3^{2+}$/DPyA could be altered within a broad range of 82 nm by facile protonation/deprotonation process of DPyA. Photophysical experiments and theoretical calculations concluded that the switch of excitation state from LE to CT was responsible for the considerable bathochromic shift upon acidification. It is noted that the proposed strategy would be suggestive for further development of reversible color-tunable TTA-UC acceptors by pairwise manipulation of the sensitizer and pH-sensitive acceptor. As a demonstration, the TTA-UC system was applied as a reliable light source to photocontrol the reversible *Z/E* isomerization reaction of hemiindigo upon low-energy excitation (638 nm). The current platform may also be applicable for biological imaging, say, clinical diagnosis of tumors, considering the weakly acidic extracellular domain of cancerous tissues.

Declaration of Competing Interest

The authors declare that they have no known competing financial interests or personal relationships that could have appeared to influence the work reported in this paper.

Acknowledgements

We gratefully acknowledge the financial support from the Natural Science Foundation of China (Grant Nos. 51903159, 51903161 and 91833304), the Shenzhen Science and Technology Program (KQTD20170330110107046), the Shenzhen

Technology and Innovation Commission (JCYJ20180507182244027), Foundation for Basic and Applied Research of Guangdong Province (2019A1515110915) and the Natural Science Foundation of Shenzhen University (Grant No. 2019001). We thank the Instrumental Analysis Center of Shenzhen University for analytical support. We also thank Prof. Henry Dube for providing us the UV-vis absorption spectra data of the Z/E geometry of hemiindigo.

References (格式还未修改，投稿前修改。)

[1] a) B. Joarder, N. Yanai, N. Kimizuka, *J. Phys. Chem. Lett.* **2018**, *9*, 4613-4624; b) X. Guo, Y. Liu, Q. Chen, D. Zhao, Y. Ma, *Adv. Opt. Mater.* **2018**, *6*, 1700981; c) T. W. Schmidt, F. N. Castellano, *J. Phys. Chem. Lett.* **2014**, *5*, 4062-4072; d) J. Perego, J. Pedrini, C. X. Bezuidenhout, P. E. Sozzani, F. Meinardi, S. Bracco, A. Comotti, A. Monguzzi, *Adv. Mater.* **2019**, *31*, 1903309.

[2] a) R. Haruki, Y. Sasaki, K. Masutani, N. Yanai, N. Kimizuka, *Chem. Commun.* **2020**, *56*, 7017-7020; b) C. Fan, L. Wei, T. Niu, M. Rao, G. Cheng, J. J. Chruma, W. Wu, C. Yang, *J. Am. Chem. Soc.* **2019**, *141*, 15070-15077; c) Y. Wei, M. Zheng, L. Chen, X. Zhou, S. Liu, *Dalton Trans.* **2019**, *48*, 11763-11771; d) Y. Wei, Y. Li, M. Zheng, X. Zhou, Y. Zou, C. Yang, *Adv. Opt. Mater.* **2020**, *8*, 1902157; e) Y. Wei, M. Zhou, Q. Zhou, X. Zhou, S. Liu, S. Zhang, B. Zhang, *Phys. Chem. Chem. Phys.* **2017**, *19*, 22049-22060; f) J. De Roo, Z. Huang, N. J. Schuster, L. S. Hamachi, D. N. Congreve, Z. Xu, P. Xia, D. A. Fishman, T. Lian, J. S. Owen, M. L. Tang, *Chem. Mater.* **2020**, *32*, 1461-1466.

[3] a) Y. Y. Cheng, B. Fückel, R. W. MacQueen, T. Khoury, R. G. C. R. Clady, T. F. Schulze, N. J. Ekins-Daukes, M. J. Crossley, B. Stannowski, K. Lips, T. W. Schmidt, *Energ. Environ. Sci.* **2012**, *5*, 6953-6959; b) S. P. Hill, K. Hanson, *J. Am. Chem. Soc.* **2017**, *139*, 10988-10991; c) S. Wieghold, A. S. Bieber, Z. A. VanOrman, L. Nienhaus, *J. Phys. Chem. Lett.* **2019**, *10*, 3806-3811; d) N. Geva, L. Nienhaus, M. Wu, V. Bulovic, M. A. Baldo, T. Van Voorhis, M. G. Bawendi, *J. Phys. Chem. Lett.* **2019**, *10*, 3147-3152.

[4] B. Shan, T. T. Li, M. K. Brennaman, A. Nayak, L. Wu, T. J. Meyer, *J. Am. Chem. Soc.* **2019**, *141*, 463-471.

[5] D. Choi, S. K. Nam, K. Kim, J. H. Moon, *Angew. Chem. Int. Ed.* **2019**, *58*, 6891-6895.

[6] H. Minami, T. Ichikawa, K. Nakamura, N. Kobayashi, *Chem. Commun.* **2019**, *55*, 12611-12614.

[7] J. Han, P. Duan, X. Li, M. H. Liu, *J. Am. Chem. Soc.* **2017**, *139*, 9783-9786.

[8] a) N. Kimizuka, Y. Sasaki, M. Oshikawa, P. Bharmoria, H. Kouno, A. Hayashi-Takagi, M. Sato,

I. Ajioka, N. Yanai, *Angew. Chem. Int. Ed.* **2019**, *58*, 17827-17833; b) M. Xu, X. Zou, Q. Su, W. Yuan, C. Cao, Q. Wang, X. Zhu, W. Feng, F. Li, *Nat. Commun.* **2018**, *9*, 2698; c) L. Huang, Zhao, Y., Zhang, H., Huang, K., Yang, J., & Han, G, *Angew. Chem. Int. Ed.* **2017**, *56*, 14400-14404; d) Q. Liu, M. Xu, T. Yang, B. Tian, X. Zhang, F. Li, *ACS Appl. Mater. Interfaces* **2018**, *10*, 9883-9888.

[9] X. Cui, J. Zhao, Y. Zhou, J. Ma, Y. Zhao, *J. Am. Chem. Soc.* **2014**, *136*, 9256-9259.

[10] a) R. Hao, C. Ye, X. Wang, L. Zhu, S. Chen, J. Yang, X.-T. Tao, *J. Phys. Chem. C* **2017**, *121*, 13524-13531; b) D. Yildiz, C. Baumann, A. Mikosch, A. J. Kuehne, A. Herrmann, R. Göstl, *Angew. Chem. Int. Ed.* **2019**, *58*, 12919-12923; c) M. P. Jewell, M. D. Greer, A. L. Dailey, K. J. Cash, *ACS Sens.* **2020**, *5*, 474-480; d) G. Massaro, J. Hernando, D. Ruiz-Molina, C. Roscini, L. Latterini, *Chem. Mater.* **2016**, *28*, 738-745.

[11] a) N. Kimizuka, K. Mase, Y. Sasaki, N. Tamaoki, C. Weder, N. Yanai, Y. Sagara, *Angew. Chem. Int. Ed.* **2018**, *130*, 2856-2860; b) H. Liu, X. Yan, L. Shen, Z. Tang, S. Liu, X. Li, *Mater. Horizons* **2019**, *6*, 990-995; c) Y. Liu, K. Chen, S. Yang, D. Zheng, G. Ren, Y. Yang, J. Zhao, D. Wei, K. Han, *J. Phys. Chem. Lett.* **2019**, 4368-4373.

[12] a) D. Asanuma, Y. Takaoka, S. Namiki, K. Takikawa, M. Kamiya, T. Nagano, Y. Urano, K. Hirose, *Angew. Chem. Int. Ed.* **2014**, *53*, 6085-6089; b) Shangfeng, Wang, Yong, Fan, Dandan, Li, Caixia, Sun, Zuhai, Lei, *Nat. Commun.* **2019**, *10*, 1-11; c) R. Hashimoto, M. Minoshima, J. Kikuta, S. Yari, S. D. Bull, M. Ishii, K. Kikuchi, *Angew. Chem. Int. Ed.* **2020**, 10.1002/anie.202006388.

[13] a) V. Gray, D. Dzebo, A. Lundin, J. Alborzpour, M. Abrahamsson, B. Albinsson, K. Moth-Poulsen, *J. Mater. Chem. C* **2015**, *3*, 11111-11121; b) Q. Zhou, M. Zhou, Y. Wei, X. Zhou, S. Liu, S. Zhang, B. Zhang, *Phys. Chem. Chem. Phys.* **2017**, *19*, 1516-1525.

[14] Y. Shen, A. J. Shuhendler, D. Ye, J.-J. Xu, H.-Y. Chen, *Chem. Soc. Rev.* **2016**, *45*, 6725-6741.

[15] C. Petermayer, S. Thumser, F. Kink, P. Mayer, H. Dube, *J. Am. Chem. Soc.* **2017**, *139*, 15060-15067.

[16] a) A. A. Beharry, O. Sadovski, G. A. Woolley, *J. Am. Chem. Soc.* **2011**, *133*, 19684-19687; b) D. Bleger, J. Schwarz, A. M. Brouwer, S. Hecht, *J. Am. Chem. Soc.* **2012**, *134*, 20597-20600; c) S. Helmy, F. A. Leibfarth, S. Oh, J. E. Poelma, C. J. Hawker, J. Read de Alaniz, *J. Am. Chem. Soc.* **2014**, *136*, 8169-8172; d) M. Borowiak, W. Nahaboo, M. Reynders, K. Nekolla, P. Jalinot, J. Hasserodt, M. Rehberg, M. Delattre, S. Zahler, A. Vollmar, D. Trauner, O. Thorn-Seshold, *Cell* **2015**, *162*, 403-411.